

V. T. Rangel-Kuoppa and J. Dekker, Deep levels in GaInNAs grown by molecular beam epitaxy and their concentration reduction with annealing treatment, *Materials Science and Engineering B* 129, 222-227 (2006).

© 2006 Elsevier Science

Reprinted with permission from Elsevier.

Deep levels in GaInNAs grown by molecular beam epitaxy and their concentration reduction with annealing treatment

V.T. Rangel-Kuoppa^{a,*}, J. Dekker^b

^a Optoelectronics Research Centre, Tampere University of Technology, P.O. Box 692, 33101 Tampere, Finland

^b VTT Information Technology, Microelectronics, Tietotie 3, P.O. Box 1208, FIN-02044 VTT, Finland

Received 15 September 2004; received in revised form 27 January 2006; accepted 28 January 2006

Abstract

Deep-level transient Fourier spectroscopy (DLTFS) technique is used to investigate the thermal-annealing behaviour of at least five deep levels in two samples of Ga_{0.987}In_{0.013}N_{0.0043}As_{0.9957}, one medium doped with Si ($2 \times 10^{16} \text{ cm}^{-3}$) and the second one heavily doped with Si ($1 \times 10^{18} \text{ cm}^{-3}$) grown by molecular beam epitaxy (MBE). The thermal-annealing study was done at 650, 700, 750 and 800 °C for 5 min. One main electron trap with activation energy of 0.97 eV, a capture cross section of $5.5 \times 10^{-11} \text{ cm}^2$ and a density of $3.2 \times 10^{14} \text{ cm}^{-3}$ is detected for the medium-doped as-grown sample. For the heavily doped sample one main electron trap with activation energy of 0.35 eV, a capture cross section of $7.1 \times 10^{-14} \text{ cm}^2$ and a density of $2.2 \times 10^{15} \text{ cm}^{-3}$ is detected. For the heavily doped sample, this electron trap only decreases its density as the annealing temperature increases. No more deep centres appear with annealing. For the medium-doped sample, the main electron trap decreases its density as the annealing temperature increases, but unlike the heavily doped sample, four more deep centres appear, depending on the annealing temperature. Their annealing temperature dependence and possible origin of the electron traps are reported for the first time.

© 2006 Elsevier B.V. All rights reserved.

Keywords: GaInNAs; DLTFS; Deep level; Annealing treatment

GaInNAs has recently attracted attention as a promising material to achieve 1.3 or 1.55 μm lasers for optical fiber communication systems [1,2], heterojunction bipolar transistors [3] and high-efficiency solar cells [4–6] due to its low band gap and lattice matching to GaAs [7,8]. Because it is still a relatively new material [7,8] many of its electrical properties remain unknown, although post-growth annealing is known to have a major effect on the materials performance [9–11]. However, optimisation of growth and annealing of GaInNAs faces some challenges [12]. In particular, low growth temperatures are needed for efficient incorporation of nitrogen, yet this leads to defects such as cation vacancies [13], which require annealing. This annealing, in turn, is limited to low temperatures due to In or anion diffusion [14]. Previously, empirically optimised growth and anneal temperatures for GaInNAs quantum wells samples have been found based on photoluminescence studies [14]. There-

fore, a study of deep levels and their annealing behaviour is essential.

In this work, the behaviour of the deep levels in GaInNAs with low In and N composition are studied to facilitate the comparison with GaAs [15] results in the literature. Although this approach is very similar to the one made by Polyakov et al. [9], our results are very different. They use a sample with 1% In and 0.35% N and similar doping ($7 \times 10^{16} \text{ cm}^{-3}$) but they find only two deep levels. In our work we find five deep levels. Also our work reports for the first time to our knowledge the behaviour of these levels following annealing at a range of temperatures.

In this paper we study n-type Ga_{0.987}In_{0.013}N_{0.0043}As_{0.9957} medium Si doped ($2 \times 10^{16} \text{ cm}^{-3}$) and heavily Si doped ($1 \times 10^{18} \text{ cm}^{-3}$) grown by gas source molecular beam epitaxy (GSMBE) lattice matched to GaAs. Nitrogen is provided by an RF-coupled plasma and other details of the growth may be found in Ref. [12]. Deep-level transient Fourier spectroscopy (DLTFS) is used for studying the electrical properties. The samples were grown 2-μm thick grown on an n-type GaAs (100) substrate. GaInAs single quantum wells (SQW) 7 nm thick were grown to calibrate the In composition, by comparing dynamical theory

* Corresponding author at: Optoelectronics Laboratory, Helsinki University of Technology, P.O. Box 3500, Helsinki, FIN-02015 HUT, Finland. Tel.: +358 94515362; fax: +358 94513128.

E-mail address: tapio.rangel@hut.fi (V.T. Rangel-Kuoppa).

simulations with experimental double crystal X-ray diffraction (XRD) rocking curves. The N growth was calibrated by lattice matching the GaInNAs with the substrate. This was verified by XRD.

The thermal treatment consisted on 5 min annealing for 650, 700, 750 and 800 °C in a thermal-annealing (TA) furnace under flowing nitrogen. In order to avoid out-diffusion, the samples were capped with 200 nm SiO₂ deposited by plasma-enhanced chemical vapor deposition at 300 °C for 2 min before the thermal treatment.

For the DLTFs study a Biorad 8600 DLTFs device was used. Schottky contacts were made from 100 nm of evaporated Au using a lift-off process. The area of the Schottky contact was $2.38 \times 10^{-3} \text{ cm}^2$. An ohmic contact on the backside of the substrate was made by evaporating multiple metal layers of 5 nm Ni/5 nm Au/30 nm Ge/100 nm Au, and then annealing the contact for 1 min at 410 °C. The diodes had an ideality factor of $n = 1.3$ when measured at room temperature. The reverse bias used for the DLTFs testing was limited by the low breakdown voltage of the diodes, which occurred around -1.0 V . The DLTFs measurements were made using a reverse bias of -0.7 V and a pulse voltage of 0 V . The pulse was applied during 100 ms, after which the change in capacitance was measured for 10 ms.

From the DLTFs spectra (Fig. 1) it is possible to see that up to five different deep levels appear during the annealing process. For each of these peaks, it was found that the capture cross section, measured during isothermal scans, varied by less than 3%, indicating that the activation energies determined from the Arrhenius plot are reliable. For the as-grown (■) sample, deep-level A is at 380 K. For temperatures below this, the absolute value of the leakage currents (Fig. 1) are approximately or less than $1 \mu\text{A}$. However, after annealing at 700 °C (+), 750 °C (◁) and 800 °C (×) the leakage current during the measurement of peak A has approached $10 \mu\text{A}$. As a result, the requirements for thermodynamic equilibrium described by Lang [16] may no longer be valid. Nevertheless, Arrhenius fits (Fig. 2) to the emission data for peak A gave good results, yielding an activation energy (E_A) of 0.97 eV, a capture cross section (σ_{DL}) of $5.5 \times 10^{-11} \text{ cm}^2$ and a density (ρ_{DL}) of $3.2 \times 10^{14} \text{ cm}^{-3}$. The evolution of these parameters with the annealing temperature can be seen in Figs. 3 and 4. The values for ρ_{DL} , σ_{DL} and E_A with their precisions and related significant numbers are given in Appendix A. Only parameters with good correlation values (>0.9) are given. Another factor which may hinder the regression is the influence of the overlapping peak B, which increases as the peak A amplitude decreases due to the anneals. To our knowledge this is the first time it is reported for this material. The concentration of peak A is reduced by annealing so we presume it is due to some point defect or point defect/impurity complex. If a comparison is made with GaAs, the peak has similar temperature and energy to the EL2 defect according to the nomenclature proposed by Martin et al. [15], This is usually assigned to the native arsenic antisite [17] (As_{Ga}).

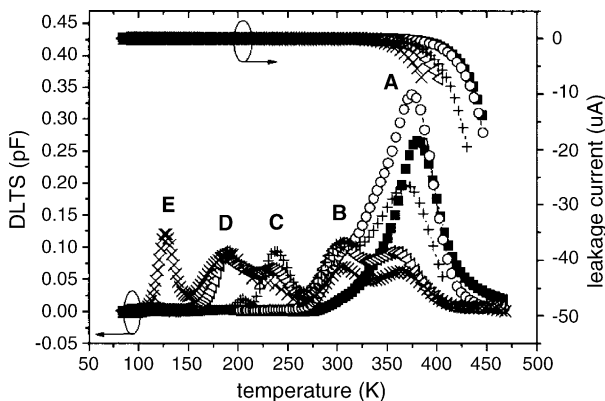


Fig. 1. DLTS spectra and leakage current of Ga_{0.987}In_{0.013}N_{0.0043}As_{0.9957} medium Si doped measured with a pulse width of 100 ms, a period width of 10 ms and a voltage of -0.7 V . The graphics correspond to following thermal-annealing temperatures: (■) none, (○) 650 °C, (+) 700 °C, (◁) 750 °C and (×) 800 °C.

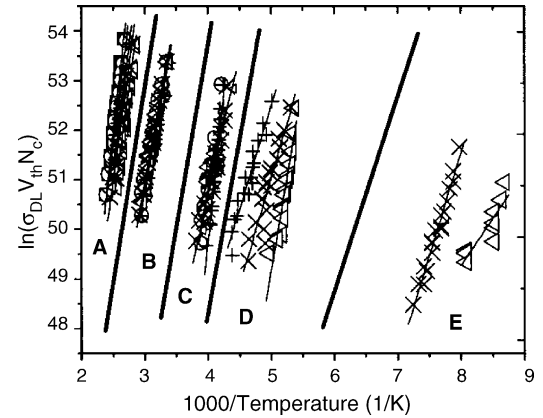


Fig. 2. Arrhenius plot for traps A–E. N_C is the effective density of states, v_{th} is the mean thermal velocity and σ_{DL} is the capture cross section. The graphics correspond to following thermal-annealing temperatures: (■) none, (○) 650 °C, (+) 700 °C, (◁) 750 °C and (×) 800 °C. The annealing time was 5 min. The thick lines are used to separate the respective group of data for each deep level.

vation energy (E_A) of 0.97 eV, a capture cross section (σ_{DL}) of $5.5 \times 10^{-11} \text{ cm}^2$ and a density (ρ_{DL}) of $3.2 \times 10^{14} \text{ cm}^{-3}$. The evolution of these parameters with the annealing temperature can be seen in Figs. 3 and 4. The values for ρ_{DL} , σ_{DL} and E_A with their precisions and related significant numbers are given in Appendix A. Only parameters with good correlation values (>0.9) are given. Another factor which may hinder the regression is the influence of the overlapping peak B, which increases as the peak A amplitude decreases due to the anneals. To our knowledge this is the first time it is reported for this material. The concentration of peak A is reduced by annealing so we presume it is due to some point defect or point defect/impurity complex. If a comparison is made with GaAs, the peak has similar temperature and energy to the EL2 defect according to the nomenclature proposed by Martin et al. [15], This is usually assigned to the native arsenic antisite [17] (As_{Ga}).

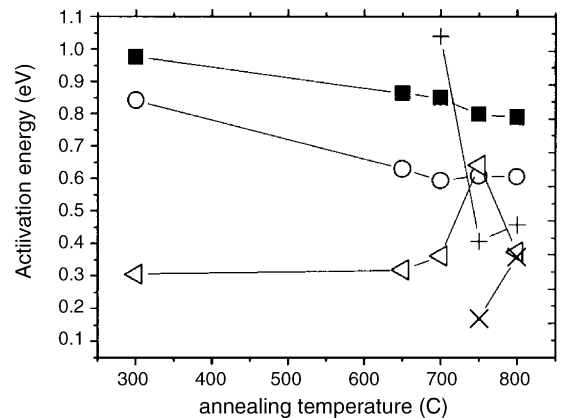


Fig. 3. Evolution of activation energy E_A for traps A (■), B (○), C (+), D (◁) and E (×) respect to annealing temperature. The annealing time was 5 min. The data plot at 410 °C represent the as-grown material, which has been annealed for the ohmic contacts.

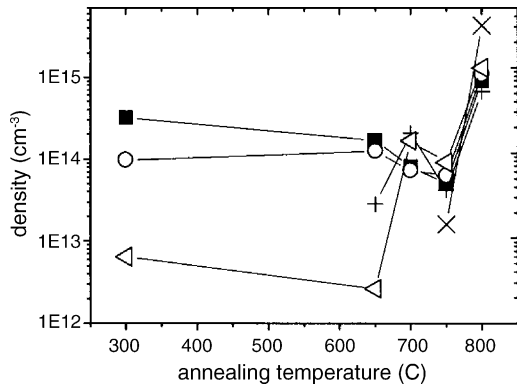


Fig. 4. Evolution of density ρ_{DL} for traps A (■), B (○), C (+), D (◁) and E (×) respect to annealing temperature. The annealing time was 5 min. The data plot at 410 °C represent the as-grown material, which has been annealed for the ohmic contacts.

Peak B appears as a small shoulder on peak A for the as-grown sample, becoming a more prominent shoulder after 650 °C annealing until it finally separates completely after a 700 °C anneal (+). Its activation and cross section are in the range of 0.59 eV and $1 \times 10^{-13} \text{ cm}^2$, respectively. As can be seen from Fig. 4, its concentration is relatively unaffected by annealing until temperatures of 800 °C at which point it increases dramatically. This deep level also appears in a similar study [18] we have done on $\text{Ga}_{0.986}\text{In}_{0.014}\text{As}$ with a similar E_A but with a ρ_{DL} two orders of magnitude bigger. Watson et al. [19] observed two similar overlapping traps and associated one of them, with $E_A = 0.58 \text{ eV}$, with misfit dislocations. When comparing the GaInAs results with the data for GaInNAs, a reduction in misfit dislocation density is expected as the N should help with strain compensation. On the other hand, Polyakov et al. [9] associated this defect with EL3, arguing that its origins are due to off-center substitutional oxygen atoms on As sites. Such an origin cannot be ruled out since oxygen can be supplied by, among other things, decomposition of the SiO_2 layer or impurities in the N_2 source. Balcioglu et al. [20] have reported an oxygen-related defect with a similar activation energy in material grown by metal organic chemical vapor deposition (MOCVD) used for solar cells. A reduction in concentration may then be seen if N is able to hinder the incorporation of O in the crystal, very possibly taking its place as both atoms have very similar dimensions and are just different by one electron.

Deep-level C appears only after 700 °C annealing, but the calculated E_A , σ_{DL} and ρ_{DL} for this annealing temperature gave unrealistic values. This deep level cannot be correlated with any level on the same study [18] done on $\text{Ga}_{0.986}\text{In}_{0.014}\text{As}$. It might be comparable with EL5 in GaAs [15]. Polyakov et al. [9] did not report this level in their GaInNAs sample, but they saw it for their GaAsN sample. On the other hand, Markov et al. [21] have reported the presence of EL5 in GaAs grown by vertical Bridgman (VB) but not by liquid encapsulated Czochralski (LEC). Dislocation densities around 10^3 cm^{-2} can be easily obtained by VB technique [22]. If it is assumed that N incorporation in GaAs generates dislocations, which are reduced if In is simul-

taneously added, then this suggests a relation between peak C (and EL5) in GaAs, GaNAs and GaInAs. This too might involve dislocations, possibly as the N moves out of its substitutional positions [23] or as it forms In–N bonds [24]. This assumption is also supported by the work of Ashizawa et al. [25] and Watson et al. [19] They found deep centres in lattice-mismatched GaInAs/GaAs interfaces caused by misfit dislocations, with activation energies between 0.49 and 0.58 eV, close to our values.

Deep-level D appears after an annealing of 700 °C, and continues for 750 and 800 °C. It is similar to the EL6 defect of GaAs [15]. Polyakov et al. [9] reported the presence of this level in GaAs, GaNAs and GaInNAs. In their study, the level peak was intense for the GaAs sample, decreases for GaAsN, and was the weakest for GaInNAs. This means that the defect is intrinsic to GaAs and the fact it appears with annealing could indicate that In or N atoms are moving to interstitial positions or clustering and leaving vacancies and GaAs clusters behind.

Finally, deep-level E appears after annealing at 750 °C. The activation energy and capture cross-section could not be realistically calculated, although simulations indicate an energy in the region of 0.25 eV (assuming $\sigma_{DL} = 1 \times 10^{-14} \text{ cm}^{-2}$). The concentration is around $1.6 \times 10^{13} \text{ cm}^{-3}$. It shows a more prominent peak for 800 °C annealing, but again the calculated parameters are unrealistic. The peak temperature makes it appear similar to the EL10 defect [15]. This level has been previously reported in the literature for GaAs [21,22] and it appears for As-rich samples. This suggests that for this annealing temperature, excess As defects such as interstitials or anti-sites may be occurring. It is also possible that V_{Ga} are formed, and As clusters there. There appear to be other smaller peaks at other temperatures, but they are disregarded because their parameter calculations turned out to have very poor correlation factor. On the $\text{Ga}_{0.986}\text{In}_{0.014}\text{As}$ study [18], we found a deep level with a similar $E_A \sim 0.2 \text{ eV}$, which appears on as-grown and all annealed samples, with a ρ_{DL} practically constant. This suggests that it is not related at all with N.

Regarding the heavy-doped sample, in Fig. 5 the DLTS spectrum is shown.

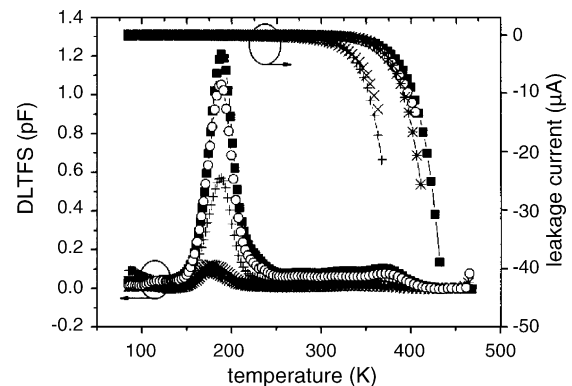


Fig. 5. DLTS spectra and leakage current of $\text{Ga}_{0.987}\text{In}_{0.013}\text{N}_{0.0043}\text{As}_{0.9957}$ heavily Si doped measured with a pulse width of 100 ms, a period width of 10 ms and a voltage of -0.7 V . The graphics correspond to following thermal-annealing temperatures: (■) none, (○) 650 °C, (+) 700 °C, (×) 750 °C and (*) 800 °C.

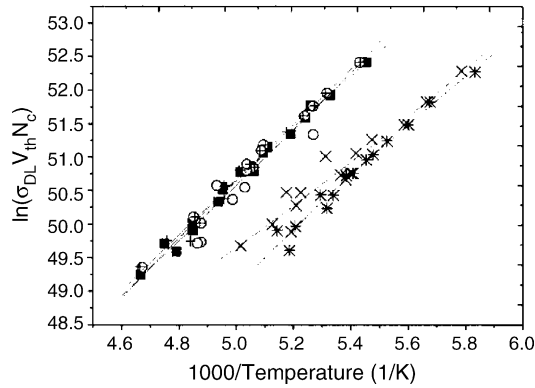


Fig. 6. Arrhenius for the deep-level D found in the $\text{Ga}_{0.987}\text{In}_{0.013}\text{N}_{0.0043}\text{As}_{0.9957}$ heavily Si-doped sample. N_C is the effective density of states, v_{th} is the mean thermal velocity and σ_{DL} is the capture cross section. The graphics correspond to following thermal-annealing temperatures: (■) none, (○) 650 °C, (+) 750 °C, (<) 750 °C and (×) 800 °C. The annealing time was 5 min.

Clearly only peak D appears. The Arrhenius plot is shown in Fig. 6.

The evolution of E_A and ρ_{DL} parameters can be seen in Fig. 7. The activation energy presents a sudden drop for 750 °C. It is very similar to the value obtained for the medium Si-doped sample. It is interesting to note that the density decreases for higher annealing temperatures. An effect totally opposite as seen for the medium Si-doped sample. An opposite behaviour is seen for the medium Si doped, where annealing at higher temperatures increases the density of deep centres.

The studied thickness for both samples was calculated from the measured capacitance at reverse bias and pulse bias, as function of temperature. It is shown in Fig. 8.

It is clear that for the medium-doped sample, the bulk material is studied in the temperature range where deep levels appear (100–450 K). On the other hand, for the heavy-doped sample, on the temperature range where the peak appears (150–250 K) only a small layer close to the surface is studied. Then, this level might be related to surface states, very likely to Ga or As broken bonds, due to the small In and N content. This gives support for the former interpretation of deep-level D on the medium-doped sample.

Previously [13], PA measurements revealed that Ga vacancy concentration are higher in nitride-containing GaInNAs compared to GaInAs, possibly due to implant-related damage from

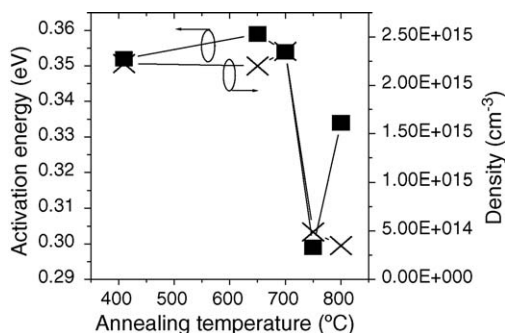


Fig. 7. Evolution of the activation energy and density of $\text{Ga}_{0.987}\text{In}_{0.013}\text{N}_{0.0043}\text{As}_{0.9957}$ heavily Si doped.

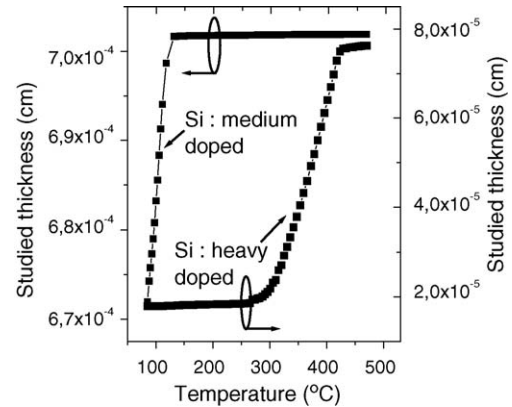


Fig. 8. Studied thickness of $\text{Ga}_{0.987}\text{In}_{0.013}\text{N}_{0.0043}\text{As}_{0.9957}$ medium and heavily Si doped, as a function of temperature. The studied thickness was calculated from the capacitance measured at reverse and pulse bias.

energetic N-ions. These defects were removed by annealing at 750 °C. Polyakov et al. [9] also observed an increase in the intensity of broad photoluminescence band associated with Ga vacancies in GaAsN relative to GaAs. The observations of increased EL2 and EL6 concentrations and of Ga vacancy-related defects in the GaInNAs, compared to GaInAs may support that, since they are known to be generated by irradiation damage in GaAs [26]. GaInAs studied earlier contained only small EL6 [18]. With regards to the annealing behaviour of these levels, anneals below 700 °C appear to have very little impact on the defect concentrations. The deepest level observed in this work, possibly EL2, drops in concentration at higher temperatures but samples degradation (poor correlations fits) reduce the confidence. Likewise, peak D, possible EL6, also drops in concentration. Polyakov et al. [9] identified EL3 as an important recombination centre. If its origins truly lie with oxygen, then the slight reduction seen in its concentration after annealing at relatively high temperatures must be due to clustering or other rearrangements.

In summary, the thermal-annealing behaviour of $\text{Ga}_{0.987}\text{In}_{0.013}\text{N}_{0.0043}\text{As}_{0.9957}$ medium Si doped and heavy Si doped have been studied by DLTS. It was found that there are up to five electron traps, some of which can be compared to well-known deep levels in GaAs. For the medium-doped sample, peak A is the main level for the as-grown sample, which might be related to the native arsenic antisite (As_{Ga}) such as EL2 in GaAs [27]. Peak B is almost not affected by thermal annealing. Comparison with the study of the $\text{Ga}_{0.986}\text{In}_{0.014}\text{As}$ study [18] shows it is not related with N and it is very likely related with the off-center substitutional oxygen in As sites. Peak C appears only after annealing at 750 °C and then is almost not affected by higher annealing temperatures. Comparison with the study of the $\text{Ga}_{0.986}\text{In}_{0.014}\text{As}$ study [18] suggests N is involved, maybe because GaNAs and GaInAs clustering, which generates local dislocations. Peak D appears for 750 °C annealing and is almost not affected by higher annealing. It has been reported to be intrinsic to GaAs but we found it is constant on $\text{Ga}_{0.986}\text{In}_{0.014}\text{As}$, which suggest N is not involved on it, but As interstitials and antisites. N might hinder the presence of these As defects. This peak is the only one which appears for the heavy Si-doped sample. Finally peak E is seen

only for an 800 °C annealing. This level is scarcely reported in the literature. It cannot be reliably evaluated and we assume it is due to high disorder introduced in the material due to the high annealing temperature.

Further research is necessary to clarify the role of heavy Si doping to avoid deep levels in GaInNAs.

Acknowledgements

We are grateful to S. Karirinne, T. Jouhti and J. Kontinen for growing the samples. Special gratitude is expressed to H. Lipsanen and M. Sapanen for their scientific opinion. This work was supported, in part, by the Academy of Finland within the framework of the DIODE Project and by the National Council for Science and Technology (CONACYT) of Mexico, Fellowship 136605.

Appendix A

A.1. DLTFs calculated parameters via Arrhenius plot for the medium Si-doped Ga_{0.987}In_{0.013}N_{0.0043}As_{0.9957} (all annealing times are 5 min)

A.1.1. Trap A: The maximum errors for E_A, σ_{DL} and ρ_{DL} are 3.3, 8.1 and 9.3%, respectively

Annealing temperature (°C)	Activation energy (E _A) (eV)	Capture cross section (σ _{DL}) (cm ²)	Density (ρ _{DL}) (cm ⁻³)	Correlation
As-grown	0.97	5.5 × 10 ⁻¹¹	3.2 × 10 ¹⁴	0.99756
650	0.86	2.5 × 10 ⁻¹²	1.7 × 10 ¹⁴	0.99237
700	0.85	2.8 × 10 ⁻¹²	8 × 10 ¹³	0.965
750	0.79	1.3 × 10 ⁻¹²	5 × 10 ¹³	0.97878
800	0.79	6.2 × 10 ⁻¹³	9 × 10 ¹⁶	0.98264

A.1.2. Trap B: The maximum errors for E_A, σ_{DL} and ρ_{DL} are 4.1, 9.3 and 10.1%, respectively

Annealing temperature (°C)	Activation energy (E _A) (eV)	Capture cross section (σ _{DL}) (cm ²)	Density (ρ _{DL}) (cm ⁻³)	Correlation
700	0.59	8.5 × 10 ⁻¹⁴	7.3 × 10 ¹³	0.98493
750	0.6	1.2 × 10 ⁻¹³	6.4 × 10 ¹³	0.99485
800	0.6	1 × 10 ⁻¹³	1.1 × 10 ¹⁵	0.99732

A.1.3. Trap C: The maximum errors for E_A, σ_{DL} and ρ_{DL} are 4.4, 9 and 9.7%, respectively

Annealing temperature (°C)	Activation energy (E _A) (eV)	Capture cross section (σ _{DL}) (cm ²)	Density (ρ _{DL}) (cm ⁻³)	Correlation
750	0.4	1 × 10 ⁻¹⁴	4.2 × 10 ¹³	0.9051
800	0.46	1.6 × 10 ⁻¹³	6.6 × 10 ¹⁴	0.94345

A.1.4. Trap D: The maximum errors for E_A, σ_{DL} and ρ_{DL} are 4.5, 9.6 and 11.2%, respectively

Annealing temperature (°C)	Activation energy (E _A) (eV)	Capture cross section (σ _{DL}) (cm ²)	Density (ρ _{DL}) (cm ⁻³)	Correlation
700	0.36	2 × 10 ⁻¹⁴	1.7 × 10 ¹⁴	0.96384
800	0.37	1.7 × 10 ⁻¹³	1.3 × 10 ¹⁵	0.92644

A.2. DLTFs calculated parameters via Arrhenius plot for the heavy Si-doped Ga_{0.987}In_{0.013}N_{0.0043}As_{0.9957} (all annealing times are 5 min)

A.2.1. Trap D: The maximum errors for E_A, σ_{DL} and ρ_{DL} are 5.4, 10.1 and 11.7%, respectively

Annealing temperature (°C)	Activation energy (E _A) (eV)	Capture cross section (σ _{DL}) (cm ²)	Density (ρ _{DL}) (cm ⁻³)	Correlation
As-grown	0.35	7.1 × 10 ⁻¹⁴	2.2 × 10 ¹⁵	0.9965
650	0.36	9.7 × 10 ⁻¹⁴	2.2 × 10 ¹⁵	0.99429
700	0.35	7.8 × 10 ⁻¹⁴	2.3 × 10 ¹⁵	0.99596
750	0.3	9.5 × 10 ⁻¹⁵	4.9 × 10 ¹⁴	0.97477
800	0.33	1.2 × 10 ⁻¹³	3.4 × 10 ¹⁴	0.99111

References

- [1] M.C. Larson, M. Kondow, T. Kitatani, K. Tamura, Y. Yazawa, M. Okai, IEEE Photonics Technol. Lett. 9 (1997) 1549.
- [2] M. Kondow, T. Kitatani, M.C. Larson, K. Nakahara, K. Uomi, H. Inoue, J. Cryst. Growth 188 (1998) 255.
- [3] S.J. Pearton, F. Ren, A.P. Zhang, K.P. Lee, Mater. Sci. Eng. R30 (2000) 55.
- [4] S.R. Kurtz, A.A. Allerman, E.D. Jones, J.M. Gee, J.J. Banas, B.E. Hammons, Appl. Phys. Lett. 74 (1999) 729.
- [5] D.J. Friedman, J.F. Geisz, S.R. Kurtz, J.M. Olson, J. Cryst. Growth 195 (1998) 409.
- [6] R.J. Kaplar, D. Kwon, S.A. Ringel, A.A. Allerman, S.R. Kurtz, E.D. Jones, R.M. Sieg, Solar Energy Mater. Solar Cells 69 (2001) 85.
- [7] M. Kondow, K. Uomi, A. Niwa, T. Kitatani, S. Watahiki, Y. Yazawa, Solid State Device Mater. (Osaka) (1995) 1016.
- [8] M. Kondow, K. Uomi, A. Niwa, T. Kitatani, S. Watahiki, Y. Yazawa, Jpn. J. Appl. Phys. 35 (1996) 1273.
- [9] A.Y. Polyakov, N.B. Smirnov, A.V. Govorkov, A.E. Botchkarev, N.N. Nelson, M.M.E. Fahmi, J.A. Griffin, A. Khan, S.N. Mohammad, D.K. Johnstone, V.T. Bublik, K.D. Chsherbachev, M.I. Voronova, V.S. Kasatochkin, Solid-State Electron. 46 (2002) 2155.
- [10] A.J. Ptak, S.W. Johnston, S. Kurtz, D.J. Friedman, W.K. Metzger, J. Cryst. Growth (available online 24 December 2002).
- [11] R.J. Kaplar, S.A. Ringel, S.R. Kurtz, J.F. Klem, A.A. Allerman, Appl. Phys. Lett. 80 (2002) 25.
- [12] H.F. Liu, S. Karirinne, C.S. Peng, T. Jouhti, J. Kontinen, M. Pessa, J. Cryst. Growth 263 (2004) 171.
- [13] W. Li, M. Pessa, T. Ahlgren, J. Decker, Appl. Phys. Lett. 79 (2001) 1094.
- [14] Y. Fedorenko, T. Jouhti, E.-M. Pavelescu, S. Karirinne, J. Kontinen, M. Pessa, Thin Solid Films 440 (2003) 195.
- [15] G.M. Martin, A. Mitonneau, A. Mircea, Electron. Lett. 13 (1977) 191.
- [16] D.V. Lang, J. Appl. Phys. 45 (1974) 3023.
- [17] R.R. Sumathi, M. Udhayasankar, J. Kumar, P. Magudapathy, K.G.M. Nair, Physica B 308–310 (2001) 1209.
- [18] V.T. Rangel-Kuoppa, J. Dekker, Mater. Sci. Eng. B, in press.

- [19] G.P. Watson, D.G. Ast, T.J. Anderson, B. Bathangey, Y. Hayakawa, J. Appl. Phys. 71 (1992) 3399.
- [20] A. Balcioglu, R.K. Ahrenkiel, D.J. Friedman, Appl. Phys. Lett. 76 (2000) 17.
- [21] A.V. Markov, A.Y. Polyakov, N.B. Smirnov, Y.N. Bolsheva, A.V. Govorkov, B.N. Sharonov, Solid-State Electron. 46 (2002) 269.
- [22] H. Nakanishi, H. Kohda, J. Cryst. Growth 155 (1995) 171.
- [23] W. Li, J. Turpeinen, P. Melanen, P. Savolainen, P. Uusimaa, M. Pessa, Appl. Phys. Lett. 78 (2001) 1.
- [24] S. Kurtz, J. Klem, A. Allerman, R. Sieg, C. Seager, E. Jones, Appl. Phys. Lett. 80 (2002) 1379.
- [25] Y. Ashizawa, S. Akbar, W.J. Schaff, L.F. Eastman, E.A. Fitzgerald, D.G. Ast, J. Appl. Phys. 64 (1988) 4065.
- [26] S.T. Lai, D. Alexiev, B.D. Nener, J. Appl. Phys. 78 (1995) 3686.
- [27] D.V. Lang, A.Y. Cho, A.C. Gossard, M. Ilegems, W. Wiegmann, J. Appl. Phys. 47 (1976) 2558.